

Self-Calibration for Industrial Robots with Rotational Joints

K. Radkhah*

Department of Computer Science,
Technische Universität Darmstadt, Darmstadt, Germany
E-mail: radkhah@sim.tu-darmstadt.de

*Corresponding author

T. Hemker

Department of Computer Science,
Technische Universität Darmstadt, Darmstadt, Germany
E-mail: hemker@sim.tu-darmstadt.de

O.v. Stryk

Department of Computer Science,
Technische Universität Darmstadt, Darmstadt, Germany
E-mail: stryk@sim.tu-darmstadt.de

1 INTRODUCTION

This paper describes the procedure, methodology and results of static calibration of an extended parametric forward kinematic model for industrial robots with rotational joints using a simple CCD camera. We present a novel problem formulation for the occurring positioning deviations avoiding three disadvantages inherent to the existing approaches: (1) the use of additional external measuring systems, (2) the use of the internal robot error model, and (3) the difficult, time-consuming and cost-intensive determination of the robot base.

Absolute accuracy of industrial robots is required in various applications. Accurate manipulators can be installed as measuring tools, e.g. in the area of mounting and spot-welding of bodywork. The capturing of welded points by so called control robots represents an important area of application. Incorrectly welded points and their late notice lead to problems and delay times of the production. Therefore, it is highly important to notice such problems early in the production process. Recently an even higher tendency towards the replacement of machine and special tools by industrial robots can be observed. Figure 1 shows the in-line measurement cell for car body inspection with KUKA KR45 robots.

Reliable and fast warning systems, though, require absolutely accurate robots. Hardware modification, i. e., revising the robot mechanical structure or design and imposing tighter tolerances in manufacturing the robot parts, is one common way to improve the accuracy of industrial robots. Considering economical criteria, however, it is a more cost-effective solution to build a manipulator with relaxed tolerances and to modify the mathematical model in the controller, i. e., to achieve high accuracy

through software rather than hardware modification.

This method is a useful tool and widely known as robot calibration. It is a very practical problem facing those involved in the implementation of advanced automation. After calibration, often a drastic improvement of almost two orders of magnitude can be reported, for instance from 1 cm down to 0.2 mm (Wiest, 2001). Robot calibration methods can be distinguished into three types:

- Error Registration, i. e., the identification of deviations from the nominal behavior without assigning them to error sources. The robot acts as a black box system, where a command pose in Cartesian space is entered and an attained pose is received. If the observed Cartesian values do not correspond to the desired ones, the Cartesian deviations are stored in a kind of look-up table. The robot error for any command pose can be predicted through interpolation and then compensated for.
- Static calibration, i. e., identification of an accurate model covering all the physical properties and effects that influence the static and time-invariant positioning accuracy of the manipulator.
- Dynamic calibration, i. e., identification of the dynamic model including all motion characteristics of the manipulator (forces, actuator torques, accelerations) and dynamic effects that occur on a manipulator, such as friction and link stiffness.

This work conducts a feasibility study on achieving absolute positioning accuracy through static calibration. To the best of

our knowledge, there exists currently no experimental setup that facilitates the use of an industrial robot as a measuring instrument without the requirement of an external measuring system. To achieve this goal, we performed the necessary steps common to calibration procedures, also shown in Figure 2: modeling, measuring, identifying the parameters, compensating the errors, and validating the results. The structure of the paper is as follows. In Section 2 we present a short survey of the existing calibration approaches including the experimental setups. Section 3 introduces the developed parametric model that takes into account the geometric and nongeometric effects of the structure of an industrial robot. The developed problem formulation as well as the different calibration methodologies depending on the amount of existing absolutely accurate measurement data: one-, three- and six-dimensional calibration and the subsequent parameter identification are the focus of Section 4. Numerical aspects and optimization issues, such as optimal starting values, are the subject of Section 5. The replicated experimental setup consisting of an industrial robot, a CCD camera, and several calibration objects is discussed in Section 6. The simulation of the setup and the numerical results of the application of the developed calibration procedure to a typical industrial robot are outlined in Section 7. Finally we analyze the obtained results and the achieved accuracies.

2 STATE OF THE ART

For calibration, so-called kinematic-loop methods, introduced by Hollerbach and Wampler (1996), are used by most research groups and implemented by many commercial calibration packages. Kinematic-loop methods can be applied with a variety of TCP measurement options (Hollerbach and Wampler, 1996). These methods can be divided into three different groups:

- Open-loop methods are applied to setups where an external metrology system measures the complete or partial end point pose of an end effector. Hereby, the number of measured pose components can vary from just one component of pose to six (full pose). By moving all joints, individual poses are attained. The kinematic parameters are determined from a nonlinear optimization of the total pose set (Mooring, Roth, and Driels, 1991). In general, the term open-loop refers to an end point that is positioned freely in space.
- In closed-loop methods calibration is performed using only joint angle sensing, without any external measuring system (Bennett, Hollerbach, and Geiger, 1991).
- Screw-axis measurement methods identify individual joint axes as lines in space, i. e., an analytical solution to the kinematic parameters is possible.

In reality, though, the distinction among these methods is often small and arbitrary. By considering the external measuring system as forming a joint that closes the base with the end effector, all methods can be considered as closed-loop methods (Wampler and Arai, 1992).

The goal of the measurement is to determine accurately the complete end effector pose or some subset of the pose for a particular set of robot joint angles. The result of the measurement process is thus the collection of data sets containing the joint displacements and some portion of the end effector pose for a number of robot configurations for the parameter identification.

There are different approaches for position measurement with industrial robots: touching reference parts, using supersonic distance sensors, laser interferometers, theodolites, calipers or laser triangulation. In general, the measurement devices and techniques always differ depending on the necessary mathematical model's set of parameters that need to be identified. They also differ because of the wide variety of sizes and geometries with which robots are commercially available. Furthermore, the measurement devices change with the amount of calibrated dimensions. In other words, they are structured according to the amount of obtained pose. These mutual dependencies are also shown in Figure 3. The used measuring system should ideally be at least one order of magnitude more accurate than the device being calibrated and at least two orders of magnitude more accurate than the desired accuracy of the robot calibration.

Obviously, the less dimensions are calibrated the more data is necessary to correctly identify the robot's model. An ideal measuring system would acquire the position and orientation of the manipulator since this would incorporate the maximum information for each position of the arm (Driels, Schwayze, and Potter, 1993). Therefore, particularly the use of a 6D measurement system based on a contact-less principle is recommended (Schröer, 1998). Of course the more data is calibrated the more the computation time increases. Despite higher computation time, though, it is clear that the higher the number of calibrated dimensions the better the results will be due to the higher amount of information of the measurement data.

To avoid the use of a separate measuring system, in many robotics based applications it is preferred to use robots as measuring systems for work-cell calibration. This solution, however, implicitly includes some important assumptions subject to the condition that the robots are not provided with a self-calibration ability which is the goal of this work. First, the visual inspection of the target points on the workpiece is the weak point of the procedure because its accuracy cannot be controlled. Second, if non-calibrated robots are used, then the resulting transformation between workpiece reference frame and robot base incorporates a local approximation of all robot errors. In some cases, this is desired because the achieved accuracy may be sufficient for a certain robot task.

To conclude, there is no "best" measurement system for robot calibration. The appropriate measurement device needs to be selected regarding the desired precision and the planned cost of the system. The most desirable system represents the best compromise between cost, ease of use, and precision for a given calibration task. Existing calibration techniques, no matter how sophisticated, make use of external measuring systems, i.e. a laser tracker that measures the position and orientation of the end effector w. r. t. the robot base, as demonstrated in Figure 4.

Both internal and external metrology equipment is essential as it determines the problem formulation for the parameter identification of the robot whereas the parameter identification

method is essential for retrieving the errors in the parameters. The identification procedure computes those model parameters \mathbf{v}^* that result in an optimal fit between the actually measured position and that computed by the model. An investigation of various options for formulating an objective function that numerically solves this optimization problem leads to the conclusion to use least-squares or modifications of the least-squares method that are effected by scaling and probabilistic considerations. Usually, the objective function is defined as the error between the pose \mathbf{x}^{model} predicted by the internal model and the real pose $\mathbf{x}^{measured}$ determined by using external measurement devices:

$$\min_{\mathbf{v}} \sum_{j=1}^{n_m} \left\| \mathbf{x}_j^{measured} - \mathbf{x}^{model}(\mathbf{v}, \mathbf{q}_j) \right\|_2^2, \quad (1)$$

where n_m stands for the number of measured different joint configurations. \mathbf{q}_j denotes the vector for the configuration of all joints. In the current approaches the information of the pose contains position and orientation, only position, or only the distance of a point, mostly the end effector, w. r. t. the robot base. Note that the formulation in Equation 1 will be referred to as ‘common problem formulation’ from here onwards.

Wiest (2001) presents a 6D calibration method that requires an external measuring system. The external measuring system determines the position and orientation of an immobile calibration object w. r. t. the world frame. Other necessary measurements are performed by means of a camera system attached to the robot flange.

A different experimental setup is proposed by Beyer (2004) and Beyer and Wulfsberg (2004). The measurement tool is attached to the flange, and measures the positioning deviations from the internal robot error model in the x -, y -, and z -direction. The parameters of the kinematic model are identified by using an external measuring system.

Ji, Sun, and Yu (2007) make use of a coordinate measure machine for the robot calibration. Additionally, only geometric parameters are identified. It is stated, however, that in order to achieve better accuracy, nongeometric parameters need to be calibrated, too. Gathar et al. (2007) suggest a methodology based on a laser attached to the end effector; their approach, however, also incorporates only the geometric parameters.

The goal of this work is to provide a given robot with a self-calibration ability. The parameter identification is based on an extended accurate model that incorporates the geometric and nongeometric parameters and is carried out by means of an attached camera. Our experimental setup consists of an industrial robot with revolute joints, a camera that is attached to the robot flange, and appropriate calibration objects. The actual position of the robot flange is retrieved indirectly by the attached camera system. It is therefore not necessary that the flange is visible. In a experimental setup using an external measurement system, the flange would have had to be visible in all joint configurations. Our approach and experimental setup enable both 6D and 3D calibration. A 1D calibration is possible as well but is not expected to retrieve comparable good results as 3D or 6D calibration. When performing 1D or 3D calibration, the changing number of required measurement data needs to be considered. For 3D and 1D, the necessary measurement data set is twice and

six times as large as the measurement data set provided for 6D calibration respectively. The larger amount of data is necessary in order to keep ensuring high accuracy ranges of the results. 6D information, if not available, might be reproducible from 3D data by applying the Gram-Schmidt algorithm.

3 EXTENDED ROBOT KINEMATIC MODEL

Based on the three basic requirements completeness, model continuity, and minimality, that every kinematic model should meet (Schroer, Albright, and Grethlein, 1997), a parametric extended forward kinematic model incorporating both geometric and elastic effects for the parameter identification stage was developed. This model was introduced by Radkhah (2007) and is based on the famous *Denavit-Hartenberg* convention (Denavit and Hartenberg, 1955).

To each link i , including the end effector, with i ranging from 0 to n for an n -degrees-of-freedom (DOF) manipulator, a frame S_i is attached. The final coordinate system S_n is referred to as the end effector or tool frame. The position and orientation of a reference frame S_i w. r. t. the previous reference S_{i-1} is represented by a 4×4 homogeneous matrix ${}^{i-1}T_i^{DH}$. Each homogeneous transformation ${}^{i-1}T_i^{DH}$ is a product of four basic transformations:

$$\begin{aligned} {}^{i-1}T_i^{DH} &:= \mathbf{R}(z; o_i) \mathbf{Tr}(z; d_i) \mathbf{Tr}(x; a_i) \mathbf{R}(x; \alpha_i) \\ &= \begin{pmatrix} c_{o_i} & -s_{o_i}c_{\alpha_i} & s_{o_i}s_{\alpha_i} & a_i c_{o_i} \\ s_{o_i} & c_{o_i}c_{\alpha_i} & -c_{o_i}s_{\alpha_i} & a_i s_{o_i} \\ 0 & s_{\alpha_i} & c_{\alpha_i} & d_i \\ 0 & 0 & 0 & 1 \end{pmatrix}, \quad (2) \end{aligned}$$

with $c = \cos(\cdot)$, $s = \sin(\cdot)$. \mathbf{R} represents a rotation and \mathbf{Tr} a translation. The four quantities o_i , a_i , d_i , α_i are parameters associated with link i , $i = \{1, \dots, n\}$ and given the names *joint offset*, *link length*, *link offset* and *link twist*. To every joint i , the corresponding joint variable q_i is associated. This joint variable is either the angle of rotation in the case of a revolute joint or the joint displacement in the case of a prismatic joint, see Figure 5. The composition of all homogeneous transformations in this kinematic chain represents the relationship of a given set of joints and the position and orientation of the end effector. In our model, the joint offset o is modified to include the constant offset θ and the variable joint angle \mathbf{q} , $o_i = \theta_i + q_i$. The elements of the matrix ${}^{i-1}T_i^{DH}$ depend directly on the joint configuration parameters $\mathbf{q} \in \mathbb{R}^n$. The matrix ${}^0T_n^{DH}$, describing the position and orientation of the end effector frame w. r. t. the base frame, is formed by multiplying all ${}^{i-1}T_i^{DH}$ matrices in the kinematic chain from S_0 to S_n :

$${}^0T_n = {}^0T_1 \cdot {}^1T_2 \cdot \dots \cdot {}^{n-1}T_n.$$

In the remainder of this paper, the term *DH* within the equations is replaced by the appropriate name of the corresponding model.

We overcome the limitations of the *DH*-convention by defining and adding necessary parameters that account for the variations in the kinematic model. We take into account both geometric and nongeometric effects; particularly the elastic effects

are expected to be essential. Therefore, two parameters $s_{x,i}$ and $s_{y,i}$ describing distortions of the axis of motion z_i from its ideal orientation were included in the proposed model. Additionally, three spring constants $k_{x,i}, k_{y,i}, k_{z,i}$ representing the elastic effects in each axis of a link frame were added such that the complete extended forward kinematic model DH,s,e is formulated as:

$${}^{i-1}T_i^{DH,s,e} := \mathbf{R}(x; s_{x,i})\mathbf{R}(y; s_{y,i})\mathbf{R}(z; q_i)\mathbf{R}(z; \theta_i)\mathbf{R}(z; \gamma_{z,i}) \cdot \mathbf{R}(y; \gamma_{y,i})\mathbf{R}(x; \gamma_{x,i})\mathbf{Tr}(z; d_i)\mathbf{Tr}(x; a_i)\mathbf{R}(x; \alpha_i).$$

$\gamma_{x,i}, \gamma_{y,i}, \gamma_{z,i}$ represent the resulting rotation angles caused by the elastic deformations. For further details we refer to Radkhah et al. (2009)

Our model is similar to that proposed in Wiest (2001). However, our model experimental setups not contain the three representative orientation and translation parameters of each homogeneous transformation matrix in the forward kinematic chain. Rather the developed model exactly considers the assigned geometric and nongeometric parameters. We believe that such structured and well-developed model is of utmost importance. Particularly when considering that based on the foundations laid in this work it becomes possible to conduct further studies such as the determination of the relevant parameters to be considered by means of experiments in the compensation step.

4 PARAMETER IDENTIFICATION

The problem formulation has a great impact on the results of the calibration and depends on the experimental setup. Usually the objective function for the parameter identification of an industrial robot is formulated as the minimization of the sum of the squared differences of the measured information and the same information calculated by the developed model. Such an objective function is also known as least-squares regression function.

Existing approaches make use of an external measuring system in order to determine the robot base. A highly accurate determination of the robot base, however, is not feasible. On the other hand, the possible number of calibrated dimensions is automatically laid down by the experimental setup.

The feasibility of multi-dimensional calibration clearly depends on the used metrology system and the experimental setup as a whole. If possible a multi-dimensional calibration should be given priority to because of the obvious advantages. The most important advantage is that the calibration of n dimensions requires only $\frac{1}{n}$ of the required number of measurements for the corresponding 1D calibration. In most experimental setups, it is common to perform either a 6D or a 3D calibration. In these setups, a 6D calibration considers both the position and the orientation of the robot flange w. r. t. the robot base:

$$x^{model}(q) = \begin{pmatrix} {}^0r_n^{model} \\ \phi^{model} \\ \theta^{model} \\ \psi^{model} \end{pmatrix},$$

whereas in a 3D calibration only the position is interesting:

$$x^{model}(q) = \begin{pmatrix} {}^0r_n^{model} \end{pmatrix}.$$

x^{model} depends on the joint configuration q and denotes the position 0r_n and orientation of S_n w. r. t. frame S_0 . The orientation can be represented by Roll-Pitch-Yaw angles. This parametrization is possible for the DH-model where modeling errors are excluded. Depending on the experimental setup, the robot geometry, and the measuring systems, it is possible that besides the orientation and position of the robot flange further information is available such that even more than 6 dimensions can be considered in the formulation of the problem.

Nonetheless, the difficulties of determining the rotation angles given the rotation matrix should be taken into account. This task involved in a 6D calibration is not necessarily performed with ease since the exact and real geometry of the robot arm needs to be considered. A solution in closed-form is highly unlikely since the real model is more complex and nonlinear. Proposed methods in Sciavicco and Siciliano (1996) and Spong, Hutchinson, and Vidyasagar (2006) cannot be applied since they presume an ideal geometry of the robot arm kinematics. Furthermore, the probability of unique solutions is not ensured without any additional information from the robot controller for instance.

It should be also noted that the dimension of the problem formulation strongly depends on the accuracy of the provided information. The accuracy of the provided information is also important considering further necessary calculations. In cases where, for instance, the orientation cannot be measured directly but can be retrieved from sufficient positioning information, it is essential to determine with which accuracy these further calculations can be performed.

In this paper the presented calibration procedure is designed for 3D calibration. Considering the additional computational efforts involved in 6D calibration where the orientation of frames w. r. t. the internal camera frame needs to be calculated and hence the decreasing accuracy of computed information because of truncation and roundoff errors, it is recommendable to carry out 3D calibration.

4.1 Experimental Setup

We propose an experimental setup consisting of an industrial robot and several calibration objects (Fig. 6). The only measuring system is a camera mounted on the robot flange. The robot executes various motions based on different joint configurations. In each joint configuration, the camera records an image of a block of points. Under the circumstance that at least three points not lying on a common line are measured within the same image, the orientation of the image frame w. r. t. the camera frame can be calculated. In some cases, this information is indispensable. Therefore, it is crucial that the camera measurements are reliable and accurate.

Depending on the visual range of the attached camera, it may be possible to determine the position of points on every side of the calibration object w. r. t. the fixed internal frame. It may be also possible to generate this information by means of a reliable and accurate data sheet for the technical specification of the calibration object. Depending on the size and geometry of the robot, and the number of geometric and nongeometric parameters that need to be identified, it may be also necessary to know

the position of points on one calibration object w. r. t. positions of points on another calibration object. Depending on the area that is encircled by the calibration objects, the camera field of view may be insufficient for the determination of the connecting vectors. A once performed external measurement may be then required. However, this information can also be provided otherwise. For instance, by using a larger calibration object of a size equal to the area encircled by the smaller calibration objects, we reduce the problem to the subproblem of determining the positions of points w. r. t. the fixed internal frame. Thus, the necessary measurement data are:

- joint positions,
- position of points on the calibration objects w. r. t. the camera frame,
- position of points on the calibration objects w. r. t. the internal frame of the objects, and
- relative position of points on different calibration objects.

4.2 Novel Problem Formulation

The nonlinear least-squares regression function consists only of relative accurate data; consequently, the position of the end effector or a point on the objects w. r. t. the base frame is not measured. Instead, this information is inferred from comparing two different joint configurations that result in the same end position with minor accuracy deviations. Note that the position of points on the calibration objects within the base frame, either calculated or measured, is from here onwards also referred to as “end position”. In other words, the accurate absolute position $\mathbf{x}_j^{\text{measured}}$ (cf. Equation 1) is replaced by another calculated end position, $\mathbf{x}^{\text{model}}(\mathbf{v}, \mathbf{q}_k)$. The objective function is thus formulated as

$$\min_{\mathbf{v}} \sum_{h \in H} \rho_h \left\| \mathbf{x}^{\text{model}}(\mathbf{v}, \mathbf{q}_j) - \mathbf{x}^{\text{model}}(\mathbf{v}, \mathbf{q}_k) + \overrightarrow{UV} \right\|_2^2, \quad (3)$$

where H is the set of the different tuples $h = (k, j)$ with j and k representing two joint configurations. The weights $\rho_h > 0$ may account for measurement errors if chosen different to $\rho_h = 1$. The vector \overrightarrow{UV} represents the vector difference between the two end positions $\mathbf{x}^{\text{model}}(\mathbf{v}, \mathbf{q}_j)$ and $\mathbf{x}^{\text{model}}(\mathbf{v}, \mathbf{q}_k)$ that result out of the two joint configurations and is explained more thoroughly in the subsections below. As can be noticed from Equation (3), the sum of the differences between measured and calculated end positions is modified to the sum of the differences between two calculated end positions. This formulation involves the simultaneous consideration of two different joint configurations k and j in three operational coordinates of the above regression function. $\mathbf{q}_j, \mathbf{q}_k$ represent the two joint configurations and \mathbf{v} is the set of identification parameters. In the following we will describe more in detail the single components of the vectors $\mathbf{x}^{\text{model}}$.

4.3 Computation of the End Positions

As already mentioned, the experimental setup consists of a CCD camera attached to the end effector that measures only accurate

relative data, the position of points on the calibration objects w. r. t. the origin of the camera frame. Consequently, the positioning vectors of the end positions in Equation (3) include the information of the whole transformation chain from the robot base to the end effector

$${}^0T_n^{\text{model}} = {}^0T_1^{\text{model}} \cdot {}^1T_2^{\text{model}} \cdot \dots \cdot {}^{n-1}T_n^{\text{model}},$$

the transformation from the flange frame S_n into the camera frame S_c

$${}^0T_c^{\text{model}} = {}^0T_n^{\text{model}} \cdot {}^nT_c,$$

and the direct measurement information of the camera from the origin of the camera frame to the recorded points. Two points U and V that are measured by the camera are denoted as ${}^c\mathbf{u}$ and ${}^c\mathbf{v}$ respectively. As an example the end position of a point U with the corresponding measured positioning vector ${}^c\mathbf{u}$ can be computed w. r. t. the robot base as follows:

$$\hat{\mathbf{u}}^{\text{model}}(\mathbf{v}, \mathbf{q}_j) = {}^0T_n^{\text{model}}(\mathbf{v}, \mathbf{q}_j) {}^nT_c {}^c\hat{\mathbf{u}},$$

with $\hat{\mathbf{u}}^{\text{model}}, {}^c\hat{\mathbf{u}} \in \mathbb{R}^4$:

$$\hat{\mathbf{u}}^{\text{model}} = \begin{pmatrix} \mathbf{u}^{\text{model}} \\ 1 \end{pmatrix}, \quad {}^c\hat{\mathbf{u}} = \begin{pmatrix} {}^c\mathbf{u} \\ 1 \end{pmatrix}.$$

Further additional information and computations for the nonlinear least squares regression functions depend on the necessary calculations for the vector difference \overrightarrow{UV} and are described in the subsection below.

4.4 Computation of the Vector Difference

Depending on the measurement setup, it is possible to look at only one joint configuration, as long as it does not directly result in the same end positions. This is the case only when the camera measures the position of several points within the same joint configuration. The open chain between the calculated end positions is closed by the corresponding accurate relative position \overrightarrow{UV} respectively the connecting vector of the two points in the workspace.

In our experimental setup we differentiate between four possible tuple categories for the joint configurations:

- The end positions are located within the same image (c.f. Fig. 7).
- The end positions are located within two different images on the same side of the calibration object (c.f. Fig. 8).
- The end positions lie on two different sides on the same calibration object (c.f. Fig. 9).
- The end positions lie on two different calibration objects (c.f. Fig. 10).

To close the open chain between the points U and V within the same image, the vector connecting these points as well as the orientation of the internal frame of the calibration objects S_0 w. r. t. camera frames need to be known. This information can be retrieved by application of the Gram-Schmidt algorithm,

unless the recorded images do not contain at least three points that do not lie on the same line.

By considering configurations that result in end positions located not too close to each other, the workspace where the robot operates with high accuracy can be enlarged. Therefore, it is important to select a space-filling design of configurations in the joint value space. The importance of such space-filling design of joint configurations is also emphasized in Radkhah, Hemker, and von Stryk (2008).

5 APPROACH TO THE NUMERICAL SOLUTION

A reliable solution of the nonlinear least squares occurring in the calibration requires both well chosen initial estimates resp. boundaries and an optimal order of identification steps.

5.1 Initial Estimates and Boundaries

According to Wiest (2001) and Schröer (1993) the real positioning deviations cover a quite small range of ± 1 cm at maximum. Therefore, we use as starting values for the standard DH-parameters the nominal values provided by the manufacturer. For all other novel additional parameters such as the distortions or elastic deformations, the starting values are set to zero as these parameters are assumed not to exist in an ideal model.

Due to the small occurring positioning deviations, we set neither lower nor upper boundaries on the angular parameters. Rather, it is necessary to set boundaries on the occurring length deviations of the links since the numerical optimization method tends to compensate the positioning deviations by means of length modifications of the links (Wiest, 2001).

5.2 Sequence of Identification Steps

Simulative tests revealed that reliable results can be retrieved by the following sequence of identification steps:

1. The offsets θ_i of the joint zero positions are calibrated in a first step and then used as constants afterwards.
2. The remaining angular parameters $\alpha_i, s_{x,i}$, and $s_{y,i}$ are calibrated in a separate sequence. Their values are used as constants in the subsequent steps.
3. The elastic deformations $k_{x,i}, k_{y,i}$, and $k_{z,i}$ are determined in the third step.
4. A last step follows for the identification of the length parameters d_i, a_i . Since the length parameters change only minimally, they are released together with the above pre-calibrated parameters in the last step for identification resp. for re-identification.

This simultaneous identification in the last step is possible due to the pre-identification of the angular and the spring parameters prior to this last step. Consequently, there is no danger that runaways are produced by wrong compensation of deviations, e.g. the compensation of deviations in reality caused by the angular parameters by modifying the length parameters. Rather,

this issue occurs, if the length parameters are identified separately. The optimization algorithm might be “trapped” at local minimizers.

5.3 Jacobian of the Extended Forward Kinematic Model

In order to enhance the identification algorithm, an analytical expression for the identification Jacobian or the gradient should be included. The Jacobian J is the model function’s Jacobian containing the partial derivatives of the model parameters \mathbf{v} .

The derivation of the Jacobian or gradient is a highly time-consuming process which, however, is the price to be paid, if the application needs dictate a fast identification step. We provide an iterative method for determining the Jacobian matrix analytically by applying the chain and the product rule of differentiation and re-using the components already calculated by the forward kinematics routine.

During the identification process, Jacobian matrices w. r. t. different parameter sets are necessary. This is due to the distinguished treatment of the parameters in several identification steps. For the compensation of the errors the Jacobian matrices of the extended parameterized forward kinematic model containing the partial derivatives w. r. t. the joint configurations is required.

The partial derivatives of the parameters $\mathbf{v}_{DH,s} = \{o_i, a_i, d_i, \alpha_i, s_{x,i}, s_{y,i}\}$ of the extended model DH,s incorporating only the geometric parameters are relatively straightforward obtainable using the product rule of differentiation.

The iterative differentiation formula of the complete extended parameterized forward kinematic model for all parameters $\mathbf{v}_{DH,s,e} = \{o_i, a_i, d_i, \alpha_i, s_{x,i}, s_{y,i}, k_{x,i}, k_{y,i}, k_{z,i}\}$, however, are more difficult to obtain because the elastic deformations considered in the model depend on all parameters and the joint configurations. In other words, particularly the retrieval of the partial derivatives w. r. t. $\mathbf{v}_{DH,s}$ of the complete extended model DH,s,e involves complexity and tediousness.

The Jacobian of the extended model DH,s,e w. r. t. the calibration parameter set \mathbf{v} with $n_v = |\mathbf{v}|$ is formulated as follows:

$$J_{\mathbf{v}}^{DH,s,e} := \frac{\partial x^{DH,s,e}}{\partial \mathbf{v}} \in \mathbb{R}^{3 \times n_v}$$

where $x^{DH,s,e} \in \mathbb{R}^{3 \times 1}$. \mathbf{v} may in principle denote any combination of the standard DH-parameters $\mathbf{v}_{DH} = \{o_i, a_i, d_i, \alpha_i\}$, the distortion angles $s_{x,i}, s_{y,i}$, and the spring constants $k_{x,i}, k_{y,i}$, and $k_{z,i}$.

6 CASE STUDY

The novel problem formulation is applied to the model of a KUKA KR 125/2, an industrial robot with six revolute joints. In order to enhance the comprehensibility, a visualization tool was developed that can simulate the complete robot cell. The tool enables the observation and visibility of the robot movements to each point in Cartesian space and the calibration process. The robot is visualized through its first three joints; the

last three joints are shown as one part, i.e., axes 4, 5, and 6 are combined into the wrist.

The robot's workspace contains three calibration objects that are of similar shape as the rectangular 3D surfaces in Section 4. On every side of a calibration object, points in fixed distances of 40 mm are marked in the plain. To simplify the processing of the position of the points on the calibration objects, To each point on the calibration objects, a tuple (m, n) indicating the row m and the column n is assigned. The mounted camera completes the kinematic chain from the robot base to the measured points on the calibration objects and can be considered as 8th link connecting the robot and the calibration objects. It yields the position of the points on the calibration objects. During the recording of one image, the robot stands still. The camera records on every side six images, i.e., each of the three blocks is captured in two different joint configurations. In total 36 images are available. Every image resp. every block contains four points.

We assume the elastic deformations to be most important in the first three joints, i.e. any elastic deformations caused by the wrist, consisting of joints 4, 5, and 6, are ignored. In total, nine nongeometric and 36 geometric parameters are released for the identification.

7 NUMERICAL RESULTS

7.1 Replica of the Real Experimental Setup in Simulations

In order to examine the novel problem formulation, complete measurement data sets for the real experimental setup were generated. The idea was to obtain most realistic results from the simulations in order to facilitate the comparison of simulation and experimental results.

7.1.1 Generation of Simulation Data

The systematical generation of a complete measurement data set is given below:

- The joint angles are provided by real motion executions on the given robot in rad.
- The parameters for the transformation of the flange frame into the camera frame are also provided and assumed to be sufficiently accurate.
- The locations of the calibration objects in the robot cell are known by means of tool center point measurements with the uncalibrated robot. However, since we are aiming at sub-mm accuracies, precisely manufactured objects with previously calibrated dimensions must be used. Therefore, based on accurate position data of three corner points of a side of a calibration object w. r. t. the robot base and the production drawing, the positions of the remaining points on the calibration object are generated. This process is repeated for the other calibration objects.
- The robot specific technical data such as the DH-parameters and the dynamic parameters are provided by

the manufacturer. Various parameter settings can now be tested by modifying the values of the nominal parameters and setting possible occurring changes for the additional model parameters. The used parameter deviations are based on experiences on the approximate changes of the angular and length parameters of a typical KUKA 6-DOF industrial robot with a payload of 125 kg gained by Wiest (2001), Gräser (1999), and Schröer (1993).

- Based on the above measurement data set, the corresponding position of the points on the calibration objects within the camera frame can be determined.

Let us indicate the accuracies of the provided measurement data and the generated data:

- The joint angles are read reliably to three decimal places.
- The position of the origin of the camera frame w. r. t. the flange frame is indicated in sub- μm accuracy whereas the orientation is given in arcsec.
- The position of the points on the calibration objects is given at the range of $\pm 1\text{e-}4\text{ m}$.
- The generated camera measurements are given at the μm range.

7.1.2 Measurement Noise

Real time data series such as camera measurements often indicate an additional noise component that is subsequently overlaid. To ensure that the used algorithm is robust enough to produce highly reliable results despite the existence of measurement noise, we conduct our tests both with and without input noise on the camera measurements. The mean, variance, and distribution for the artificial noise are motivated by the assumed accuracy of appropriate CCD cameras. We test our approach with normally distributed errors with mean 0, variance $\sigma^2 = 1\text{e} - 8\text{ m}$, and standard deviation $\sigma = 1\text{e} - 4\text{ m}$. The measurement errors lie within the interval $[1\text{e-}5\text{ m}, 1\text{e-}4\text{ m}]$.

7.2 Problem Formulation for the Validation

In order to validate the novel problem formulation, we additionally make use of an external measurement system in the simulations, introducing a slightly modified nonlinear regression function. The external measurement system provides the position of the points on the calibration objects w. r. t. the robot base. This is unknown as presented in Section 4.2. An obvious advantage of such setup is the possibility of repeated calibration between the working cycles of the robot once the position of all points to be measured w. r. t. the robot base is known. We show the setup partially in Figure 11.

The position of point U is computed by:

$$\hat{\mathbf{u}}^{DH,s,e}(\mathbf{v}, \mathbf{q}_j) = {}^0T_n^{DH,s,e}(\mathbf{v}, \mathbf{q}_j)^n T_c^c \hat{\mathbf{u}}.$$

The analog measured information is represented by $\mathbf{u}_j^{measured}$. The equation for the parameter identification is similar to Equation (1):

$$\min_{\mathbf{v}} \sum_{h \in H} \left\| \mathbf{u}_j^{measured} - \mathbf{u}^{DH,s,e}(\mathbf{v}, \mathbf{q}_j) \right\|_2^2.$$

In the simulations ρ_h is set to one when measurement noise was not considered. The above problem formulation introduced for the validation can be also referred to as common problem formulation since it represents existing experimental setups.

7.3 Simulation Results

As already indicated, parameter identification for an industrial robot is not performed by simple application of an algorithm. Moreover, an optimal numerical approach is necessary for the solution of the nonlinear least squares.

We look at the identification of the extended model DH,s performed with the steps given in Table 1. The table shows the parameters released in every step, the function value at the end of every step, and the number of iterations for each step. The visualization of the real and the identified points show that the geometry of the calibration object is well identified, i.e., the function value is tried to be minimized but the identified points are displaced from the real points about a few centimeters in almost all three dimensions. The results obtained after the identification of the extended model are at least two orders of magnitude worse than the initially created deviations with the DH-model. The mean distance between the real positions and the positions computed with the DH-model deteriorates from 0.0006588 m to 0.119 m after the identification procedure. The optimization method does not find a solution in the sense of a global minimum; the positioning deviations seem to be compensated by means of length modifications of the links.

An optimal arrangement of steps is however not the only crucial factor for determining the real parameter values. We also need to increase the amount of operational coordinates of the nonlinear least-squares regression function. In total, about 3000 operational coordinates, the amount suggested by Schröder (1993) for the identification of about 45 parameters, are used. Most important, however, is the consideration of configurations that result in end positions located further away from each other, i.e., pairs of points that lie on two different calibration objects. The achieved accuracies in a run performed with the optimal order of steps and obtained with the common problem formulation with the extended model are two magnitude of orders better. The results obtained with the novel problem formulation are even slightly better than those obtained by the common formulation, see Figure 12 and Figure 13. The enlargement of the workspace, i.e. space-filling design of joint configurations, turns out to be essential, since only by the addition of pairs of points on different objects it became possible to retrieve accurate results applying the novel problem formulation. Table 2 indicates the used order of identification steps. The termination of the algorithm was based on the following conditions:

- maximum number of function evaluations allowed,
- maximum number of iterations allowed,

- tolerance on the function value $< 1e-5$ m, and/or
- tolerance on the parameter values $< 1e-6$ m resp. rad.

In order to validate the suggested problem formulation for the parameter identification, further tests were conducted with (1) different parameter values, and (2) measurement noise on the camera measurements.

Table 1: Identification of the extended model DH,s .

Step	Norm of residual	Iterations
o_i	4.5065e-6 m	6
$d_i, a_i, \alpha_i, s_{x,i}, s_{y,i}$	2.0189e-7 m	4001
$o_i, d_i, a_i, \alpha_i, s_{x,i}, s_{y,i}$	2.4874e-14 m	13

Table 2: Identification of the extended model DH,s,e .

Step	Norm of residual	Iterations
o_i	0.809270 m	9
$\alpha_i, s_{x,i}, s_{y,i}$	0.046253 m	17
$k_{x,i}, k_{y,i}, k_{z,i}$	0.043284 m	2005
$o_i, \alpha_i, s_{x,i}, s_{y,i}, k_{x,i}, k_{y,i}, k_{z,i}, d_i, a_i$	2.3396e-6 m	61

8 DISCUSSION

The above results are evaluated by estimating the accuracy that the manipulator would achieve if the identified parameters were to replace the nominal parameters in the robot control model. That means, the two forward kinematic solutions based on the actual and the standard kinematic parameters are computed. Subsequently the differential displacement is computed to determine the positioning accuracy of the calibrated manipulator. If the identified parameters result in a higher accuracy than previously achieved by the standard DH-model, then the calibration process is considered to be successfully carried out. Based on this methodology for estimating the accuracy of the obtained results, we were able to produce with both the common and novel problem formulation results within a high accuracy range. High accuracies were achieved even when measurement noise on the camera measurements was considered. Various sets of positioning deviations were tested; in all cases the identification process was carried out successfully. The end positions on the calibration objects were hit with the desired accuracy in the [1e-5 m, 1e-4 m] range. Note that this accuracy range was achieved although the actual positioning deviations prior to the parameter identification lied within the [7e-3 m, 2e-2 m] range. Consequently, a drastic improvement of at least two orders of magnitudes were achieved.

The results obtained by the common approach were expected to be precise due to the higher amount of information of measurement data input. Moreover the accuracy improvements are particularly remarkable because of the lower amount of information that characterizes the inputs of the novel problem formulation.

By applying the statistical practice of cross-validation, it could be shown that high accuracies are also achieved for joint configurations that were not considered in the calibration. Points that were not considered in the calibration were identified with almost the same accuracy as the calibrated ones. Such investigations facilitate making a statement about the workspace in which sufficiently accurate robot movements can be granted.

A failure of the identification process can be due to various reasons. It does not necessarily indicate too relaxed measurement accuracies. Furthermore, there was no evidence of run-aways in the course of iterations in none of the identification runs.

Let us summarize the important aspects that need to be considered for successfully performing a calibration:

1. optimal order for the parameter identification,
2. no separate step for the identification of length parameters,
3. enough pose measurements, and
4. enlargement of the closed kinematic chain within the operational coordinates of the regression function by selecting pairs of end positions that lie on different calibration objects.

The few requirements that need to be met by the experimental setup are:

1. a highly precise model of the calibration objects,
2. sufficiently accurate camera measurements, and
3. accurate internal sensors (such as the position encoders).

9 CONCLUSIONS

This paper presented a completely novel problem formulation facilitating an easier and a more affordable experimental setup for the calibration of industrial robots. We made use of an extended forward kinematic model taking into account both geometric and nongeometric effects. An appropriate procedure for the optimal and quick solution of the nonlinear least squares appearing in the calibration of the model parameters has been developed. Based on different experimental setups, different problem formulations have been tested and evaluated thoroughly to investigate the best method of finding an appropriate parameter set for the calibration. The tests were based on data generated for a replicated real experimental setup. The developed calibration method was applied simulatively to a typical 6-Degrees-of-freedom (DOF) industrial robot arm. The numerical results showed that the novel problem formulation can improve effectively and significantly a manipulator's accuracy without requiring cost-intensive metrology equipment. The errors between the real end positions and the end positions predicted by the standard kinematic DH-model could be decreased by at least two orders of magnitudes after application of the parameter identification with the novel problem formulation. Highly accurate results were obtained also for joint configurations that were not

considered in the calibration process. This work lays the foundations for the cost-minimal and effective realization of industrial robots as measuring instruments.

REFERENCES

- Bennett, D.J., Hollerbach, J.M. and Geiger, D. (1991) 'Autonomous Robot Calibration for Hand-Eye Coordination', *International Journal of Robotics Research*, Vol. 10, pp.550–559.
- Beyer, L. (2004) *Genauigkeitssteigerung von Industrierobotern*. PhD thesis. Universität der Bundeswehr Hamburg, Hamburg, Germany.
- Beyer, L. and Wulfsberg, J. (2004) 'Practical Robot Calibration with ROSY', *Robotica*, Vol. 22, No. 5, pp.505–512.
- Denavit, H. and Hartenberg, R.S. (1955) 'A Kinematic Notation for a Lower-Pair Mechanisms Based on Matrices', *ASME Journal of Applied Mechanics*, Vol. 22, pp.215–221.
- Driels, M.R., Schwayze, W. and Potter, S. (1993) 'Full-Pose Calibration of a Robot Manipulator Using a Coordinate-Measuring Machine', *International Journal of Advanced Manufacturing Technology*, Vol. 8, pp.34–41.
- Gathar, C.S., Lumia, R., Wood, J. and Starr, G. (2007) 'Calibration of Industrial Robots by Magnifying Errors on a Distant Plane', *Paper Presented at the 2007 IEEE/RSJ International Conference on Intelligent Robots and Systems. October 29 - November 2, 2007*. San Diego, CA, USA.
- Gräser, R.G. (1999) *Ein Verfahren zur Kompensation temperaturinduzierter Verformungen an Industrierobotern*, München: Utz Verlag.
- Hollerbach, J.M. and Wampler, C.W. (1996) 'The Calibration Index and Taxonomy for Robot Kinematic Calibration Methods', *International Journal of Robotics Research*, Vol. 15, No. 6, pp.573–591.
- Ji, J., Sun, L. and Yu, L. (2007) 'A new Pose Measuring and Kinematics Calibration Method for Manipulators', *Paper Presented at the 2007 IEEE International Conference on Robotics and Automation. April 10 - 14, 2007*. Roma, Italy.
- Lettenbauer, H. (2002) *System zum Einsatz von Industrierobotern in der fertigungsnahen Qualitätsprüfung*. PhD thesis. Universität der Bundeswehr Hamburg, Hamburg, Germany.
- Mooring, B.W., Roth, Z.S. and Driels, M.R. (1991) *Fundamentals of Manipulator Calibration*, New York: Wiley Interscience.
- Radkhah, K. (2007) *Model-Based Approach to Calibration of Industrial Robots Considering Geometric and Elastic Effects*. Diploma thesis. Department of Computer Science, Technische Universität Darmstadt, Darmstadt, Germany.

Radkhah, K., Hemker, T. and von Stryk, O. (2008) 'A Novel Self-Calibration Method for Industrial Robots Incorporating Geometric and Nongeometric Effects', *Paper Presented at the 2008 IEEE International Conference on Mechatronics and Automation*. August 5 - 8, 2008. Takamatsu, Japan.

Radkhah, K., Hemker, T. and von Stryk, O. (2009) 'Towards the deployment of industrial robots as measurement instruments - An extended forward kinematic model incorporating geometric and nongeometric effects', *Paper Presented at the 2009 IEEE/ASME International Conference on Advanced Intelligent Mechatronics*. July 14 - 17, 2009. Singapore.

Schröder, K. (1998) *Measurements and Testing: Handbook on Robot Performance Testing and Calibration: Improvement of Robot Industrial Standardisation IRIS*, Stuttgart: Fraunhofer-IRB-Verlag.

Schröder, K. (1993) *Identifikation von Kalibrationsparametern kinematischer Ketten*, München und Wien: Hanser Verlag.

Schröder, K., Albright, S.L. and Grethlein, M. (1997) 'Complete, Minimal and Model-Continuous Kinematic Models for Robot Calibration', *Robotics and Computer-Integrated Manufacturing*, Vol. 13, No. 1, pp.73-85.

Sciavicco, L. and Siciliano, B. (1996) *Modeling and Control of Robot Manipulators*, New Jersey: Mc Graw Hill.

Spong, M.W., Hutchinson, S. and Vidyasagar, M. (2006) *Robot Modeling and Control*, John Wiley and Sons.

Wampler, C. and Arai, T. (1992) 'Calibration of Robots having Kinematic Closed Loops using Non-Linear Least-Squares Estimation', *Paper Presented at the 1992 IFTOMM Symposium*. September 1 - 4, 1992. Nagoya, Japan.

Wiest, U. (2001) *Kinematische Kalibrierung von Industrierobotern*, Aachen: Shaker Verlag.

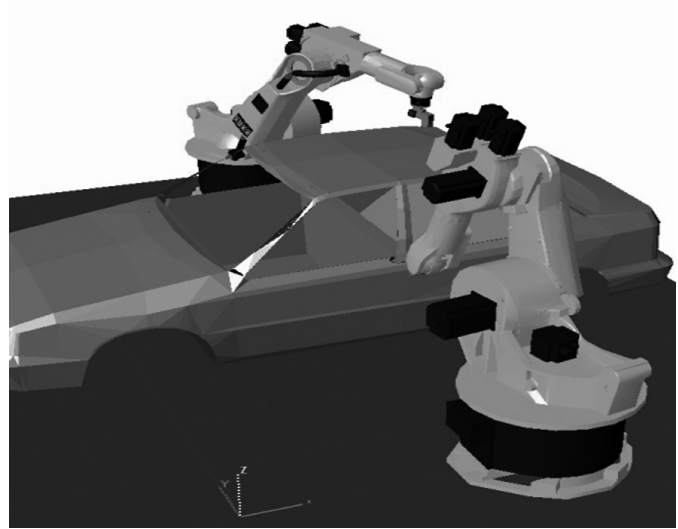


Figure 1: In-line measurement cell for car body inspection with KUKA KR 45 Robots (Lettenbauer, 2002).

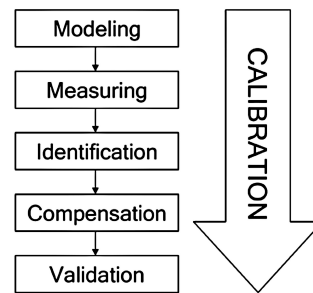


Figure 2: The developed calibration approach consists of the stages: Modeling, measuring, identification, compensation, and validation.

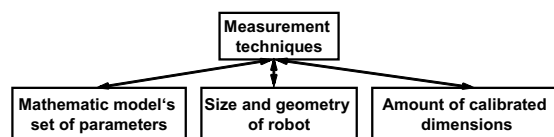


Figure 3: Important aspects to be considered when selecting the measurement techniques and devices.

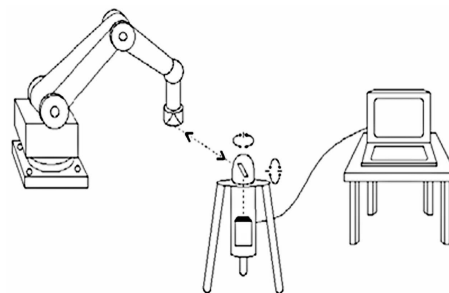


Figure 4: Laser tracker measuring the position and orientation of the end effector w.r.t. the robot base frame (Beyer, 2004).

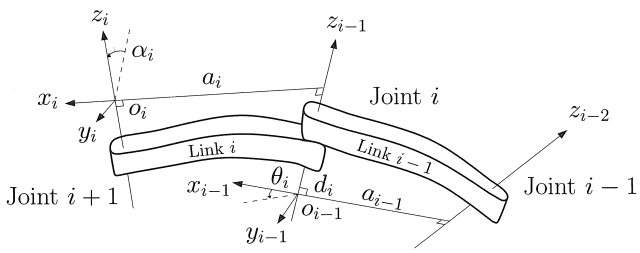


Figure 5: Denavit-Hartenberg frame assignment (Spong, Hutchinson, and Vidyasagar, 2006).

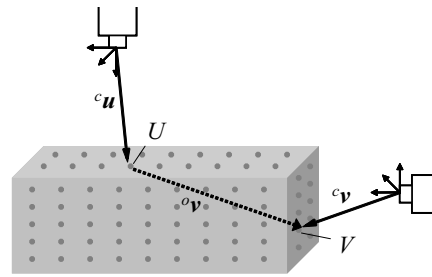


Figure 9: 3) Case: End positions lie on different sides of the calibration object.

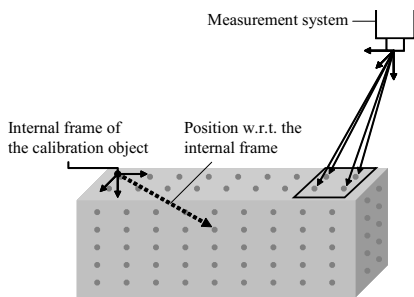


Figure 6: Measurement system records an image of one block of four points on the considered calibration object.

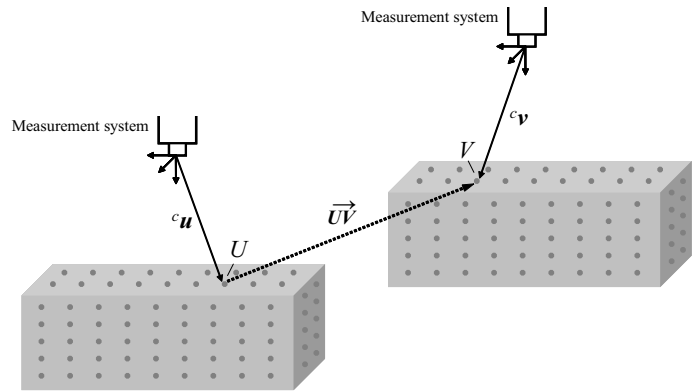


Figure 10: 4) Case: The end positions lie on different calibration objects.

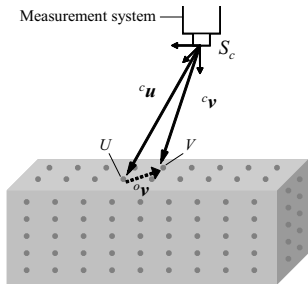


Figure 7: 1) Case: End positions lie within the same image.

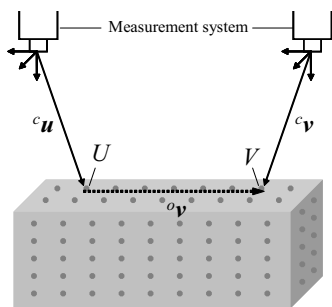


Figure 8: 2) Case: End positions lie in two different images on the same side of the calibration object.

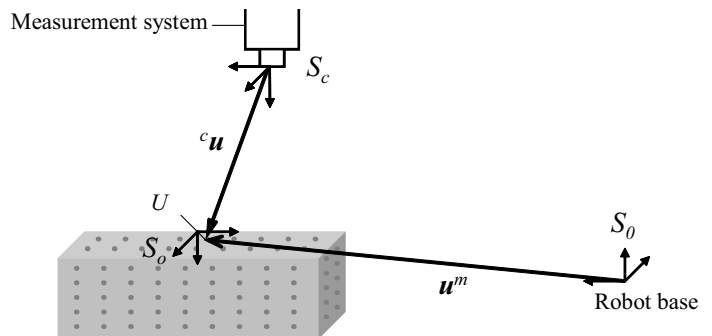


Figure 11: Position of point U on the calibration object w.r.t. the robot base is determined by an external measurement system.

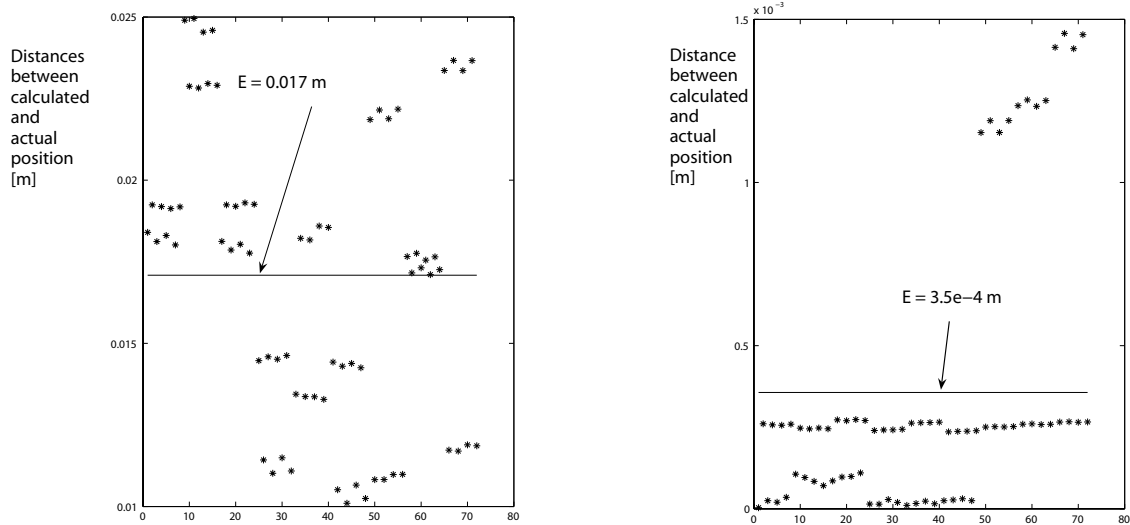


Figure 12: Comparison of obtained numerical results with the standard DH-model on the left and with the common problem formulation on the right.

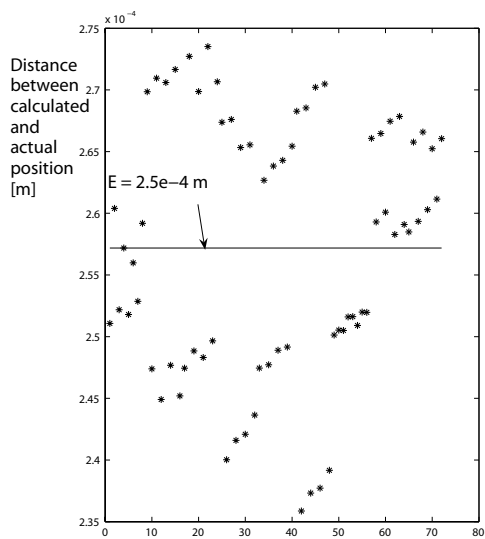


Figure 13: Results obtained with the novel problem formulation.